Exp Fluids (2015) 56:194
DOI 10.1007/s00348-015-2063-y

RESEARCH ARTICLE

Simultaneous measurements of droplet size, flying velocity and transient temperature of in-flight droplets by using a molecular tagging technique

Haixing Li[1] · Fang Chen[1,2] · Hui Hu[1]

Received: 6 March 2015 / Revised: 13 September 2015 / Accepted: 16 September 2015 / Published online: 29 September 2015

Abstract In the present study, a molecular tagging technique is introduced to achieve simultaneous measurements of droplet size, flying velocity and transient temperature of in-flight liquid droplets in a spray flow. For the molecular tagging measurements, a pulsed laser is used to "tag" phosphorescent 1-BrNp·Mβ-CD·ROH triplex molecules premixed within liquid droplets. After the same laser excitation pulse, long-lived laser-induced phosphorescence is imaged at two successive times within the phosphorescence lifetime of the tagged phosphorescent triplex molecules. While the sizes of the droplets are determined quantitatively based on the acquired droplet images with a precalibrated scale ratio between the image plane and the object plane, the displacement vectors of the in-flight droplets between the two image acquisitions are used to estimate the flying velocities of the droplets. The simultaneous measurements of the transient temperatures of the in-flight droplets are achieved by taking advantage of the temperature dependence of phosphorescence lifetime, which is estimated from the intensity ratio of the acquired phosphorescence image pair of the inflight droplets. The feasibility and implementation of the molecular tagging technique are demonstrated by conducting simultaneous measurements of droplet size, flying velocity and transient temperature of micro-sized water droplets exhausted from a piezoelectric droplet generator into ambient air at different test conditions in order to characterize the dynamic and thermodynamic behaviors of the micro-sized in-flight droplets. The unsteady heat transfer process between the in-flight droplets and the ambient air is also analyzed theoretically by using a lumped capacitance method to predict the temperature changes of the in-flight water droplets along their flight trajectories. The measured temperature data are compared with the theoretical analysis results quantitatively, and the discrepancies between measurement results and the theoretical predictions are found to be within 0.80 °C.

1 Introduction

The characterization of in-flight liquid droplets in spray flows is of great interests for a wide range of engineering applications, which include combustion, spray cooling, spray drying and fire extinction. The heat and mass transfer processes from or to liquid droplets are important control variables in many of such applications. For example, the process of breaking up or atomization of liquid fuel into droplets in the form of a fine spray plays a pivotal role in improving energy efficiency and suppressing pollutant formation for various gas turbines and internal combustion (IC) engines. A detailed definition of the dynamic and thermodynamic behaviors of in-flight fuel droplets is essential for the optimization of liquid fuel injectors/atomizers in order to maximize energy efficiency, minimize pollutant emissions and meet the operability requirements of a particular application (Schulz and Sick 2005). Spray cooling, as an effective technique to remove heat from a hot surface, has been used widely to control quenching rates in metallurgical industry (Hall and Mudawar 1995) and to achieve fast cooling of hot electronic components (Salazar et al. 2004). As reported in González and Black (1997), while the size and initial temperature of liquid droplets influence the

✉ Hui Hu
huhui@iastate.edu

[1] Department of Aerospace Engineering, Iowa State University, Ames, IA 50010, USA

[2] School of Aeronautics and Astronautics, Shanghai Jiao Tong University, Shanghai 200240, China

amount of sensible heating that can be removed in spray cooling, the behavior of the small in-flight liquid droplets would be affected by the rising hot gas or vapor resulting from the evaporation at the hot surface, inhibiting any sub-cooling effect. Thus, the quantitative information to describe the dynamic and thermodynamic characteristics of the small in-flight droplets is indispensable for the design optimization to augment the heat transfer from the hot surface in spray cooling applications.

The dynamic and thermodynamic characteristics of in-flight droplets in spray flows are usually quantified in the terms of droplet size, flying velocity and temperature of the droplets. While the size and flying velocity of liquid droplets may affect the heat and mass transfer processes between the droplets and the surrounding gas flows via convection, droplet temperature is actually one of the most important properties, which is directly related to the heat and mass transfer from or to the liquid droplets through atomization or/and evaporation process. Among various parameters of interest in characterizing the dynamic and thermodynamic behaviors of droplets in spray flows, droplet temperature is the one of the least investigated due to the lack of suitable non-intrusive measurement techniques.

Global rainbow thermometry (GRT) technique, which is based on the rainbow position and its dispersion as a function of the refractive index dependent on temperature, has been developed to measure the size and temperature of liquid droplets in spray flows (van Beeck and Riethmuller 1995; van Beeck et al. 1999). Since liquid droplets are assumed to be perfectly spherical in GRT, non-spherical droplets may cause significant systematic errors in GRT measurements (van Beeck et al. 1999; Vetrano et al. 2005). While Wilms et al. (2008) proposed an approach to improve GRT technique by filtering out the non-spherical droplets to reduce biased errors, the inevitable presence of refractive index gradients induced by the non-uniform temperature distributions within liquid droplets would still cause significant biased errors in GRT measurements (van Beeck and Riethmuller 1995; van Beeck et al. 1999).

Laser-induced fluorescence (LIF) technique has also been used for temperature measurement of liquid droplets in spray flows. LIF-based thermometry techniques are based on the temperature dependence of LIF intensity for some fluorescent tracer molecules premixed within the liquid droplets. In applying LIF-based thermometry techniques to measure temperature of liquid droplets, two detecting bands from the fluorescence spectra (i.e., two-color LIF-based thermometry) were usually chosen in order to minimize the effects of the non-uniformities of the illuminating laser intensity and fluorescence dye concentration on the temperature measurements (Lavieille et al. 2001; Castanet et al. 2002; Zhang et al. 2013). To implement two-color LIF-based thermometry techniques, two cameras with various optical filters are usually required, along with a very careful image registration or coordinate mapping procedure in order to get the quantitative spatial relation between the two acquired LIF images. In addition, other complications also need to be carefully considered, such as the relatively low temperature sensitivity, the spectral conflicts to cause reabsorption of fluorescent emission, and photobleaching of the fluorescence dyes in using two-color LIF-based thermometry approaches for the temperature measurements of in-flight droplets (Coppeta and Rogers 1998; Lavieille et al. 2001; Zhang et al. 2013).

While several other measurement techniques, which include Raman scattering (Schweiger 1990; Müller et al. 2000; Hopkins et al. 2003), thermochromic liquid crystal thermometry (Nozaki et al. 1995; Richards et al. 1998; Mochizuki et al. 1999) and infrared imaging thermography (Tuckermann et al. 2005; Wulsten and Lee 2008), have also been used to measure the temperatures of liquid droplets, almost all of them have relatively poor measurement accuracy and require complicated experimental setup to achieve quantitative temperature measurements of small in-flight liquid droplets. More recently, Lemoine and Castanet (2013) provide a comprehensive review of various optical techniques for quantitative measurements of temperature and chemical composition of droplets.

Simultaneous measurements of droplet size, flying velocity and transient temperature of in-flight droplets are highly desirable to characterize the dynamic and thermodynamic behaviors of liquid droplets in spray flows. While some of the measurement techniques described above can measure the droplet size and temperature of the liquid droplets in spray flows, none of those techniques can provide quantity measurements of the flying velocity of the in-flight droplets simultaneously. Those techniques are required to combine with other velocimetry techniques such as laser Doppler velocimetry (LDV) or particle imaging velocimetry (PIV) in order to achieve simultaneous measurements of droplet size, flying velocity and temperature of the liquid droplets in spray flows, which would complicate the experimental setup and add extra burdens on the instrumentation cost for the measurements.

In the present study, we report the progress made in our recent efforts to develop a novel molecular tagging technique for simultaneous measurements of droplet size, flying velocity and transient temperature of liquid droplets in spray flows. The molecular tagging technique described here is a laser-induced phosphorescence (LIP)-based technique, which can be considered an extension of the molecular tagging velocimetry and thermometry technique developed by Hu and Koochesfahani (2006). For the molecular tagging measurements, a pulsed laser is used to "tag" phosphorescent tracer molecules premixed within liquid droplets (i.e., water droplets for the

present study). The long-lived LIP emission is imaged at two successive times after the same laser excitation pulse. The size of the liquid droplets is determined quantitatively based on the acquired droplet images with a precalibrated scale ratio between the image plane and the object plane. A particle-tracking algorithm is used to determine the displacement vectors of the in-flight droplets between the two LIP image acquisitions, thereby, to estimate the flying velocities of the liquid droplets. The transient temperature of the in-flight droplets is derived by taking advantage of the temperature dependence of the phosphorescence lifetime, which is estimated from the phosphorescence intensity ratio of the droplets in the two interrogations.

It should be noted that, while molecular tagging techniques have been developed and successfully applied to achieve flow velocity and temperature measurements in single-phase flows (Gendrich et al. 1997; Hu and Koochesfahani 2011) and stationary surface droplets (Hu and Huang 2009; Hu and Jin 2010), the work presented here will deal with a multiphase spray flow system involving in-flight liquid droplets with transient temperature change and unsteady heat transfer with ambient gas-phase flows. The work described here, to our knowledge, is the first of its nature that is capable of achieving simultaneous measurements of droplet size, flying velocity and transient temperature of in-flight liquid droplets in spray flows. No similar work has ever been published/reported before. It can be implemented with only a single intensified CCD camera, a single-pulsed ultraviolet (UV) laser and phosphorescent molecules for the simultaneous measurements of multiple important properties in spray flows, which offers significant advantages over other flow diagnostic techniques to characterize spray flows.

In the following sections, the technical basis of a lifetime-based molecular tagging thermometry (MTT) technique for the transient temperature measurements of in-flight droplets is described briefly at first. Then, the related physical properties of the phosphorescent 1-BrNp·Mβ-CD·ROH triplex for the molecular tagging measurements are introduced. The feasibility and implementation of the molecular tagging technique are demonstrated by conducting simultaneous measurements of droplet size, flying velocity and transient temperature of micro-sized water droplets exhausted from a piezoelectric droplet generator into ambient air at different test conditions in order to characterize the dynamic and thermodynamic behaviors of the micro-sized in-flight droplets. The unsteady heat transfer process between the in-flight droplets and the ambient air is also analyzed theoretically by using the lumped capacitance method to predict the dynamic temperature changes of the in-flight water droplets along their flight trajectories. The measured temperature data are compared with the theoretical analysis results quantitatively to validate the measurement results.

2 Technical basis of the molecular tagging technique

2.1 Technical basis of molecular tagging technique for droplet temperature measurement

It is well known that both fluorescence and phosphorescence are molecular photoluminescence phenomena. Compared with fluorescence, which typically has a lifetime on the order of nanoseconds, phosphorescence can last as long as microseconds, even minutes. Since emission intensity is a function of the temperature for some substances, both fluorescence and phosphorescence of tracer molecules may be used for temperature measurements. While fluorescence (LIF) techniques have been widely used for temperature measurements of liquid droplets in spray flows (Lavieille et al. 2001; Castanet et al. 2002; Zhang et al. 2013), laser-induced phosphorescence (LIP) techniques have also been suggested recently to conduct temperature measurements of "in-flight" or levitated liquid droplets (Omrane et al. 2004a, b). Compared with LIF-based thermometry techniques, the relatively long lifetime of LIP has been used to prevent interference from scattered/reflected light and any fluorescence from other substances (such as from solid surfaces for the near-surface measurements) that are present in the measurement area, by simply putting a small time delay between the laser excitation pulse and the starting time for phosphorescence image acquisitions (Hu and Huang 2009). Furthermore, LIP was found to be much more sensitive to temperature compared with LIF (Omrane et al. 2004a, b), which is favorable for the accurate temperature measurements of small liquid droplets. The molecular tagging technique described here is a LIP-based technique.

According to quantum theory (Ramamurthy and Schanze 1998), with unsaturated laser excitation, the intensity of a photoluminescence process (either fluorescence or phosphorescence) decays exponentially. For simplicity, only a signal-exponential process is considered here. As described in Hu and Koochesfahani (2006, 2011), for a diluted solution and unsaturated laser excitation, the collected phosphorescence signal (S_p) by using a gated imaging detector with integration starting at a delay time t_o after the laser excitation pulse and a gate period of δt can be given by:

$$S_p = AI_i C\varepsilon \Phi_p \left(1 - e^{-\delta t/\tau}\right) e^{-t_o/\tau}, \quad (1)$$

where A is a parameter representing the detection collection efficiency, I_i is the local incident laser intensity, C is

the concentration of the phosphorescent dye (the tagged molecular tracer), ε is the absorption coefficient and Φ_p is the phosphorescence quantum efficiency. The emission lifetime τ refers to the time at which the intensity drops to 37 % (i.e., $1/e$) of the initial intensity. For an excited state, the deactivation processes may involve both radiative and nonradioactive pathways and the lifetime of the photoluminescence process, τ, is determined by the sum of all the deactivation rates, i.e., $\tau^{-1} = k_r + k_{nr}$, where k_r and k_{nr} are the radiative and non-radiative rate constants, respectively. According to photoluminescence kinetics, the non-radiative rate constant is, in general, temperature dependent (Ferraudi 1988), and the resulting temperature dependence of the phosphorescence lifetime is the basis of the present technique for temperature measurement.

It should also be noted that the absorption coefficient ε and quantum yield Φ_p are usually temperature dependent in general (Kim et al. 2003), resulting in a temperature-dependent phosphorescence signal (S_p). Thus, in principle, the collected phosphorescence signal (S_p) may be used to measure temperature if the incident laser intensity and the concentration of the phosphorescent dye remain constant (or are known) in the region of interest.

As shown in Eq. (1), the collected phosphorescence signal (S_p) is also a function of the incident laser intensity (I_i) and the concentration of the phosphorescent dye (C); thus, the spatial and temporal variations in the incident laser intensity and the non-uniformity of the phosphorescent dye (such as due to photobleaching and/or the changes in the dye concentration in liquid droplets during evaporation process) in the region of interest would have to be corrected separately in order to derive quantitative temperature data from the acquired phosphorescence images. In practice, however, it is very difficult, if not impossible, to ensure a non-varying incident laser intensity distribution and a constant dye concentration within liquid droplets due to evaporation process, which may cause significant errors in the temperature measurements. To overcome this problem, Hu and Koochesfahani (2003, 2006, 2011) developed a lifetime-based molecular tagging thermometry (MTT) technique, which can eliminate the effects of incident laser intensity and concentration of phosphorescent dye on temperature measurements effectively.

The lifetime-based MTT technique works as follows: As illustrated in Fig. 1, a pulsed laser is used to "tag" phosphorescent tracer molecules premixed within working liquids (i.e., water for the present study). LIP emission is interrogated at two successive times after the same laser excitation pulse. The first image is detected at the time $t = t_o$ after laser excitation for a gate period δt to accumulate the phosphorescence intensity S_1, while the second image is detected at the time $t = t_o + \Delta t$ for the same gate period to accumulate the phosphorescence intensity S_2. As described in Hu and Koochesfahani (2003, 2006, 2011), by taking

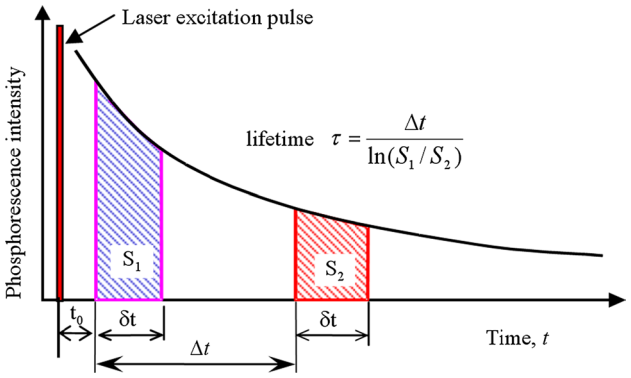

Fig. 1 Timing chart of lifetime-based MTT technique

integration of Eq. (1) on the temporal window Δt, the accumulated phosphorescence intensities S_1 and S_2 can determined, and the ratio of the two phosphorescence signals (R) can be expressed as:

$$R = S_2/S_1 = \frac{AI_i\, C\varepsilon\, \Phi_p \left(1 - e^{-\delta t/\tau}\right) e^{-(t_o+\Delta t)/\tau}}{AI_i\, C\varepsilon\, \Phi_p \left(1 - e^{-\delta t/\tau}\right) e^{-t_o/\tau}} = e^{-\Delta t/\tau}. \tag{2}$$

It indicates that the intensity ratio of the two successive phosphorescence images (R) is only a function of the phosphorescence lifetime τ and the time delay Δt between the two image acquisitions, which is a controllable parameter. Based on Eq. (2), the phosphorescence lifetime of the molecular tracers can be calculated according to

$$\tau = \frac{\Delta t}{\ln(S_1/S_2)}. \tag{3}$$

As described in Hu and Koochesfahani (2006, 2011) and Hu et al. (2010), since the photoluminescence lifetime is temperature dependent for some molecular tracers, with the conditions of diluted solution and unsaturated laser excitation, the temperature distribution in a fluid flow can be derived from the distribution of the intensity ratio of the two photoluminescence images acquired after the same laser excitation pulse. For a given molecular tracer and fixed Δt value, Eq. (2) defines a unique relation between phosphorescence intensity ratio (R) and fluid temperature T, which can be used for thermometry as long as the temperature dependence of phosphorescence lifetime of the molecular tracers is known. This ratiometric approach eliminates the effects of any temporal and spatial variations in the incident laser intensity (due to pulse-to-pulse laser energy variations) and non-uniformity of the dye concentration (e.g., due to photobleaching or concentration change in the tracer molecules within liquid droplets due to evaporation at a high-temperature environment).

To implement the lifetime-based MTT technique described above, only one laser pulse is required to excite or "tag" the tracer molecules for each instantaneous temperature measurement. The two successive acquisitions of the photoluminescence image of the tagged tracer molecules can be achieved using a dual-frame intensified CCD camera. Compared to the two-color LIF thermometry techniques described above (Lavieille et al. 2001; Castanet et al. 2002; Zhang et al. 2013), which usually require two CCD cameras with proper optical filters to acquire two fluorescent images simultaneously for each instantaneous temperature measurement, the present lifetime-based MTT technique is much easier to implement and can significantly reduce the burden on the instrumentation and experimental setup. Furthermore, since LIF emission is short lived with the emission lifetime on the order of nanoseconds, LIF images are usually acquired when the incident laser illumination is still on; therefore, they are vulnerable to the contaminations of scattered/reflected light and any fluorescence emission from other substances. For the lifetime-based MTT technique describe here, as schematically indicated in Fig. 1, the small time delay between the illumination laser pulse and the phosphorescence image acquisition can effectively eliminate all the effects of scattered/reflected light and any fluorescence from other substances that are present in the measurement region. Since only the phosphorescence emission of the tagged phosphorescent molecules was acquired for the MTT measurements, the acquired phosphorescence images of the water droplet are quite "clean," in comparison with LIF images.

2.2 Simultaneous measurements of droplet size and flying velocity of in-flight droplets

In addition to measuring the transient temperature of liquid droplets, droplet size and flying velocity of the in-flight droplets can also be determined simultaneously based on the acquired phosphorescence image pair. With a precalibrated scale ratio between the image plane and the object plane for the phosphorescence image acquisition, the size of the in-flight droplets can be determined quantitatively by measuring the dimension of the droplets in the acquired phosphorescence images via an image processing procedure. Furthermore, a particle-tracking algorithm can be used to determine the displacement vectors of the in-flight droplets between the two phosphorescence image acquisitions. Since the time delay Δt between the two image acquisitions is known for a specific experiment, the flying velocities of the in-flight droplets can also be estimated based on the measured displacement vectors of the in-flight droplets between the two phosphorescence image acquisitions.

Further technical details about the simultaneous quantification of droplet size and flying velocity, in addition to the transient temperature measurements, of the in-flight droplets will be described in the Sect. 3 of the present study.

2.3 Phosphorescence molecular tracer used in the present study

It is well known that LIP techniques usually surfer from oxygen quenching to phosphorescence emission. In the present study, a specially designed phosphorescent triplex (1-BrNp·Mβ-CD·ROH) was used as the molecular tracer for the molecular tagging measurements. The phosphorescent 1-BrNp·Mβ-CD·ROH triplex is actually the mixture compound of three different chemicals, which are lumophore (indicated collectively by 1-BrNp), maltose-β-cyclodextrin (indicated collectively by Mβ-CD) and alcohols (indicated collectively by ROH). According to Hartmann et al. (1996) and Gendrich et al. (1997), the special molecular structures of the phosphorescent triplex (1-BrNp·Mβ-CD·ROH) would form a molecular shell to prevent LIP emission of the excited 1-BrNp molecules from oxygen quenching effects.

Figure 2a shows the normalized absorption and emission spectra of the phosphorescent 1-BrNp·Mβ-CD·ROH triplex. The fluorescence and phosphorescence spectra are both shown in the plot, and the phosphorescence emission is significantly redshifted relative to fluorescence. It should be noted that, because of the large redshift as shown in the figure, there is no overlap between the phosphorescence emission and absorption spectra, which suggests that the phosphorescence does not get reabsorbed with the phosphorescent triplex (1-BrNp·Mβ-CD·ROH) as the molecular tracer for flow measurements. Figure 2b shows the emission spectra of the 1-BrNp·Mβ-CD·ROH solution at different temperatures. As shown clearly in the figure, while the phosphorescence emission of the triplex is very temperature sensitive, its fluorescence is almost independent of temperature. The fluorescence lifetime of 1-BrNp·Mβ-CD·ROH triplex is within 20 ns, while its phosphorescence lifetime is found to be much longer, on the order of several milliseconds, as reported in Hu et al. (2006) and Hu and Koochesfahani (2006, 2011). Further information about the chemical and photoluminescence properties of the phosphorescent triplex (1-BrNp·Mβ-CD·ROH) is available at Hartmann et al. (1996) and Gendrich et al. (1997).

Upon the pulsed excitation of a UV laser (i.e., quadrupled wavelength of Nd:YAG laser at 266 nm for the present study), the phosphorescence lifetime of the phosphorescent triplex (1-BrNp·Mβ-CD·ROH) molecules in an aqueous solution was found to change significantly with temperature. Figure 3 shows the measured phosphorescence lifetimes of the 1-BrNp·Mβ-CD·ROH molecules as a function

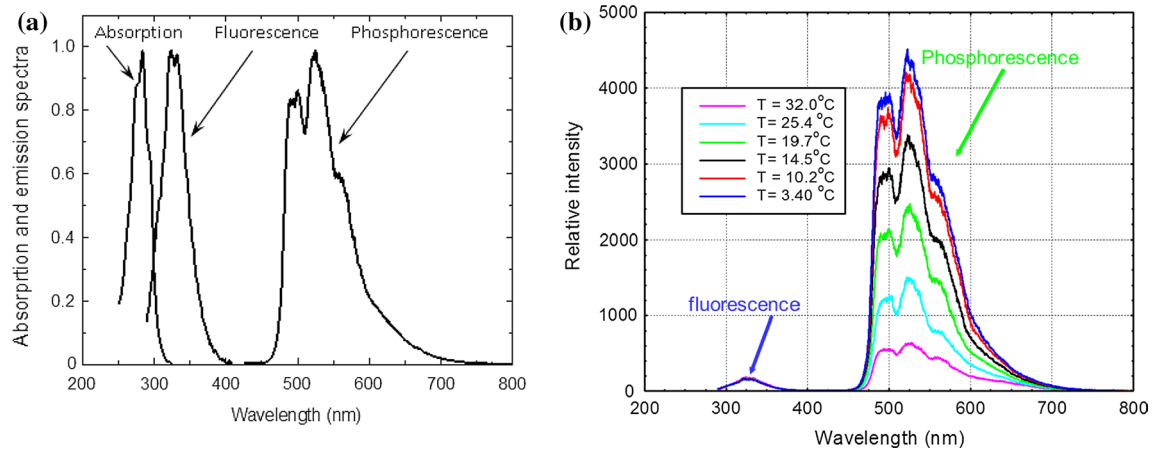

Fig. 2 Absorption and emission spectra of 1-BrNp·Gβ-CD·ROH triplex (Hu et al. 2006). **a** Normalized absorption and emission spectra, **b** emission spectra at different temperatures

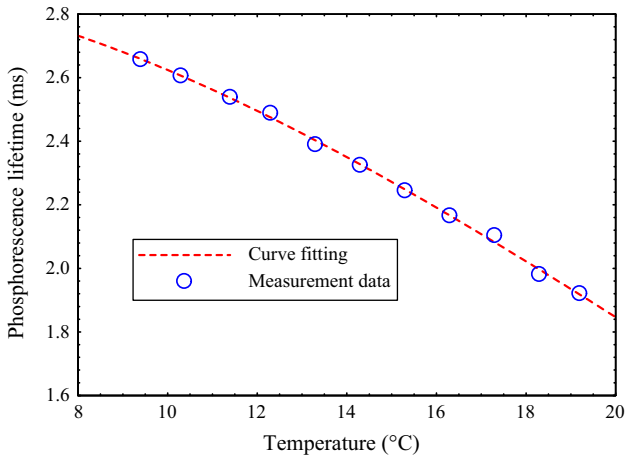

Fig. 3 Variation in droplet temperature versus phosphorescence lifetime (neopentyl alcohol was used to make 1-BrNp·Mβ-CD·ROH triplex)

of temperature, which were obtained through a calibration experiment similar as those described in Hu and Koochesfahani (2006). It can be seen clearly that phosphorescence lifetime of 1-BrNp·Mβ-CD·ROH molecules varies greatly with increasing temperature, decreasing from about 2.7 to 1.9 ms as the temperature changes from 10.0 to 20.0 °C. The relative temperature sensitivity of the phosphorescence lifetime is about 3.3 % per degree Celsius, which is much higher than that of fluorescent dyes used for LIF-based thermometry measurements. For comparison, the temperature sensitivity of Rhodamine B widely used for LIF-based thermometry is less than 2.0 % per degree Celsius (Coppeta and Rogers 1998; Hu et al. 2006).

In the present study, we used a concentration of 2×10^{-4} M for Mβ-CD, a saturated (approximately 1×10^{-5} M) solution of 1-BrNp and a concentration of 0.03 M for neopentyl alcohol (ROH) in making 1-BrNp·Mβ-CD·ROH triplex. It should be noted that, while cyclohexanol alcohol was widely used to make 1-BrNp·Mβ-CD·ROH triplex for molecular tagging measurements in the previous studies (Hu and Koochesfahani 2003; Hu et al. 2006; Hu and Jin 2010; Hu and Koochesfahani 2011), neopentyl alcohol used in the present study was found to increase the phosphorescence intensity of the 1-BrNp·Mβ-CD·ROH triplex significantly. However, the phosphorescence lifetime of 1-BrNp·Mβ-CD·ROH triplex was found to become much shorter when the neopentyl alcohol was used in making 1-BrNp·Mβ-CD·ROH triplex. For example, at the room temperature of $T = 20$ °C, the phosphorescence lifetime of 1-BrNp·Mβ-CD·ROH triplex with cyclohexanol alcohol would be about 3.7 ms as reported in Hu et al. (2010). However, it becomes only about 1.9 ms when neopentyl alcohol was used to make 1-BrNp·Mβ-CD·ROH triplex, as shown in Fig. 3.

2.4 Experimental setup for demonstration experiments

Figure 4 shows the schematic of the experimental setup used in the present study to demonstrate the feasibility and implementation of the molecular tagging technique described above to achieve simultaneous measurements of droplet size, flying velocity and transient temperature of in-flight droplets. Water is used as the working fluid in the present study, and phosphorescent triplex (1-BrNp·Mβ-CD·ROH) was premixed with water in a reservoir tank. As shown schematically in Fig. 3, a high-pressure gas cylinder was used to press the water inside the reservoir tank flow into a pipeline connected to a piezoelectric droplet generator. By applying square-wave-shaped signals to drive the piezoelectric actuator inside the droplet generator, water droplets would be generated and exhausted from the

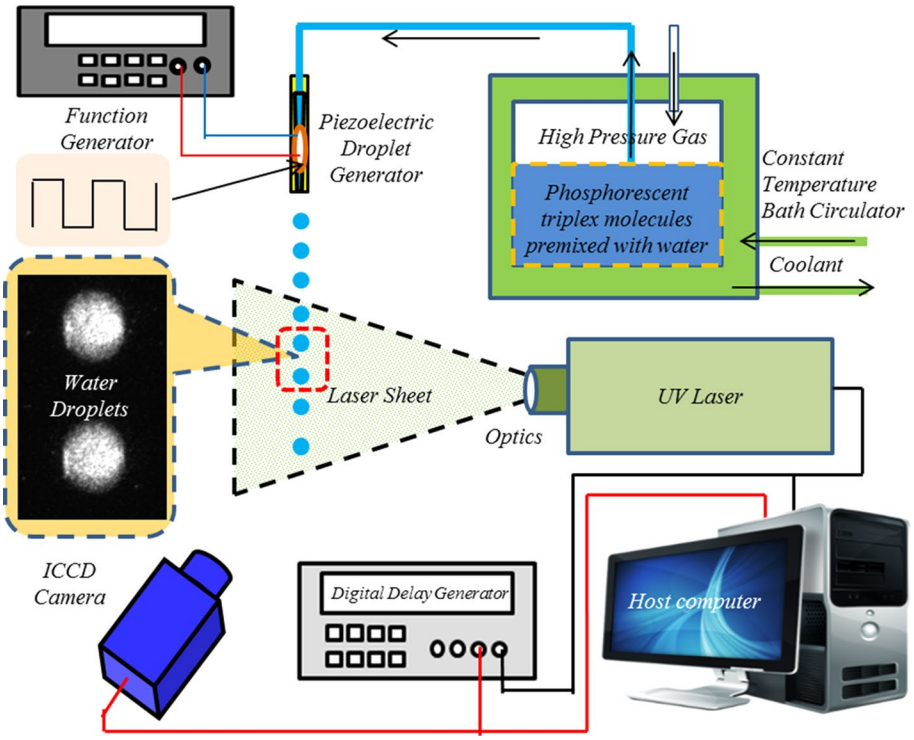

Fig. 4 Experiment setup used for the demonstration experiments

droplet generator into ambient air in a mono-sized water droplet stream. By changing the nozzle diameter of the piezoelectric droplet generator, the diameter of the water droplets exhausted from the droplet generator was adjustable in the range of 200–1000 μm (i.e., ~450 μm in diameter for the test cases of the present study). The velocity of the micro-sized water droplets exhausted from the droplet generator ranged from 0.1 to 10 m/s by varying the gas pressure applied to the water reservoir tank. During the experiments, while the temperature of the ambient air was maintained at a constant room temperature of $T_\infty = 22$ °C, the temperature of the water (i.e., along with 1-BrNp·Mβ-CD·ROH triplex) inside the reservoir tank, monitored by using a thermocouple, was kept constant at a preselected low temperature level (i.e., ranged from 3 to 15 °C) by using a constant-temperature bath circulator. As a result, the temperature of the water droplets out of the droplet generator was lower than the ambient air temperature, and the micro-sized droplets in the water droplet stream would be convectively heated up while flying in the ambient air. Thus, the temperature of the in-flight water droplets would increase monotonically along their flying trajectories.

In the present study, a pulsed Nd:YAG laser at a quadrupled wavelength of 266 nm (5-ns pulse duration) was used to excite or "tag" the molecules of 1-BrNp·Mβ-CD·ROH triplex within the water droplets. A set of optical lenses and mirrors were used to shape the laser beam into a laser sheet of ~500 μm in thickness to illuminate the mono-sized droplet stream along the central plane of the droplet generator exit. A dual-frame intensified CCD camera (PCO DICAM-Pro, Cooke Corporation, 1280 pixels × 1024 pixels in resolution) with a fast-decay phosphor (P46) was used to acquire the phosphorescence images at two successive times after the same laser excitation pulse, as shown schematically in Fig. 1. For the molecular tagging measurement results given in the present study, the first phosphorescence image of the in-flight droplets was acquired at 230 μs after the laser excitation pulse with an exposure time of 100 μs. The second phosphorescence image was acquired after the same laser pulse at 1.1 ms later with the same exposure time (i.e., $\Delta t = 1.1$ ms between the image pair). The laser and the camera were synchronized using a digital delay generator (SRS-DDG535), which controlled the timing of the laser sheet illumination and the intensified camera data acquisition.

It is also noted that since a low concentration of the phosphorescent 1-BrNp·Mβ-CD·ROH triplex was used for the present study, the effects of the molecular tracers on the physical properties of water are believed to be small and are assumed to be negligible. During the experiments, the energy level of the pulse laser used to tag the molecular tracers within water droplets was below 0.5 mJ/pulse. The repetition rate of the pulsed laser excitation was set to be 1 Hz. The energy deposited by the excitation laser into the water droplets was very small, and the temperature rise of the water droplets due to the energy deposition of the laser excitation was estimated to be very small and is also assumed to be negligible.

3 Measurement results and discussions

3.1 Determination of droplet size from the acquired phosphorescence images

As shown schematically in Fig. 1, to implement the molecular tagging technique described above, a pulsed laser was used to "tag" 1-BrNp·Mβ-CD·ROH triplex molecules premixed within the water droplets, and the "tagged" phosphorescent molecules were imaged at two successive times within the phosphorescence lifetime of the tagged tracer molecules. Figure 5 shows a typical acquired phosphorescence image pair (i.e., the first phosphorescence image was acquired at 0.23 ms after the laser excitation pulse and the second phosphorescence image at 1.33 ms after the same laser pulse with the same exposure time of 0.1 ms) for the molecular tagging measurements. It can been seen that, since the time delay (i.e., 0.23 ms for the present study) between the laser excitation pulse and the phosphorescence image acquisition can eliminate the scattered/reflected light from the droplet surfaces and any fluorescence from other substances (e.g., the transparent side walls of the test rig) near the measurement region effectively, the phosphorescence images of the water droplets are quite "clean" even though no optical filter was used in the present study for the phosphorescence image acquisition.

To implement the molecular tagging technique described above, the image size of the droplets should be consistent with the physical scale to be solved. Similar as LIF-based technique, the dynamic range of the droplet size (i.e., the range from the smallest droplet to the largest droplet) to be measured accurately is limited by the resolution of the digital camera used for the phosphorescence image acquisition. While the upper limit of the droplet size (i.e., the largest droplet to be measured accurately using molecular tagging technique) is set by the total pixel number of the digital camera, the lower limit of the droplet size (i.e., the smallest droplet to be measured accurately) is set by a single pixel of the digital camera (i.e., the water droplets with its image size being only 1 pixel in the acquired phosphorescence image).

Based on the acquired phosphorescence images as those shown in Fig. 5, the sizes of the water droplets can be measured quantitatively. Since the phosphorescence, images of the in-flight droplets are "clean," the outer boundaries of the water droplets can be identified easily in the acquired phosphorescence images by using MATLAB-based image processing software developed "in house." As shown schematically in Fig. 5a, a typical threshold intensity value of 250 for the acquired 12-bit phosphorescence images was selected in order to determine the outer boundary of a randomly selected water droplet in the droplet stream, and the diameter of the water droplet was found to be 60 pixels, i.e., $D_0 = 60$ pixels, in the acquired phosphorescence images. In the present study, a parametric study was conducted by using different threshold intensity values (i.e., the threshold intensity value was changed from 150 to 350) in identifying the outer boundaries of water droplets in the acquired 12-bit phosphorescence images. The standard deviation of the measured droplet size in the mono-sized droplet stream was found to be about 2.3 pixels, which is about 4 % of the droplet size.

With the precalibrated scale ratio between the image plane and the object plane as given in Fig. 5b, the size of the randomly selected droplet can be determined quantitatively, which was measured to be about 450 μm.

3.2 Determination of flying velocity of the in-flight water droplets

By twisting the square-wave shaped signals supplied to the piezoelectric actuator inside the droplet generator, the distance between the neighboring droplets in the droplet stream exhausted from the droplet generator can be manipulated. The information was used to identify the displacements of any preselected droplets in the mono-sized water droplet stream between the acquired phosphorescence image pair, and thereby, the flying velocity of the droplets can be determined quantitatively from the acquired phosphorescence image pair. As described above, once the outer boundaries of the droplets were determined for droplet size

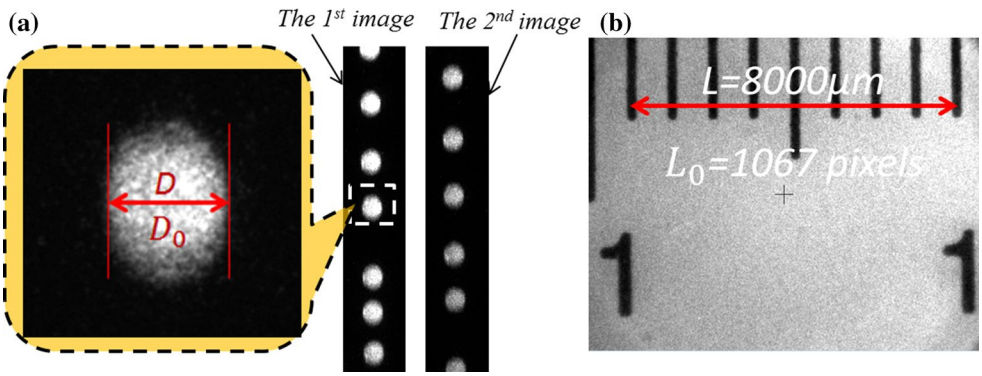

Fig. 5 Determination of droplet size from the acquired phosphorescence images. **a** Acquired phosphorescence image pair of the in-flight droplets, **b** scale ratio between the image plane and the object plane

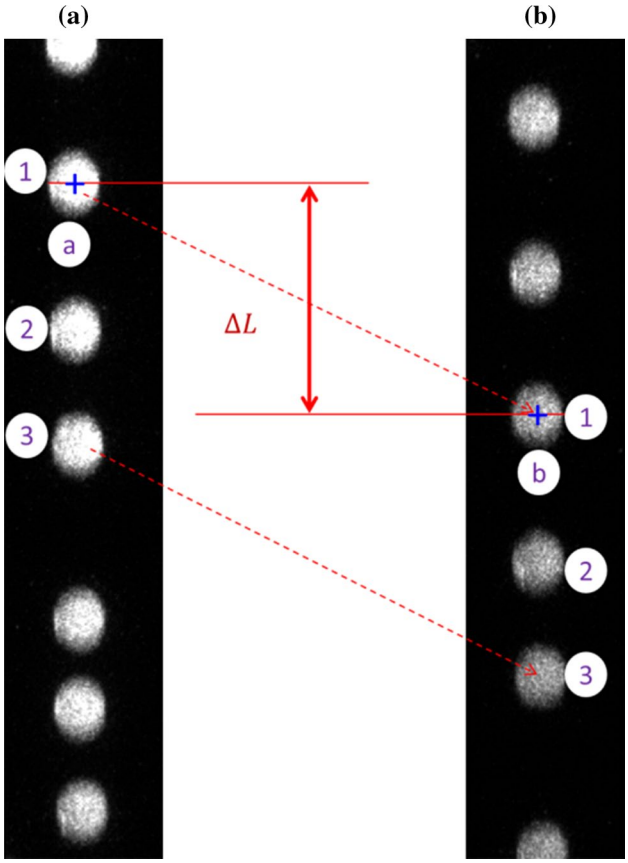

Fig. 6 Determination of the flying velocity of the droplets from the phosphorescence images. **a** The *first image* taken at 0.23 ms after the laser pulse, **b** the *second image* taken at 1.33 ms later after the same laser pulse

measurements, the center locations of the in-flight droplets in the acquired phosphorescence images as shown in Fig. 6 can be easily identified by using the MATLAB-based image processing software developed "in-house." The correspondence of the water droplets in the acquired phosphorescence image pair can be determined based on the information encoded in the distances among the neighboring droplets, which is similar to the cross-correlation-based particle-tracking algorithm used by Saga et al. (2001) for particle-tracking velocimetry (PTV) applications.

As shown schematically in Fig. 6, for a preselected droplet "#*1*" located at the position of "*a*" in the first image, the corresponding position of the same droplet, i.e., the new position "*b,*" in the second image can be determined easily based on its unique identification information encoded in the distances from the droplet to the neighboring droplets. Then, the displacement vector, $\overrightarrow{\Delta L}$, of the preselected droplet from its original position "*a*" in the first image to its new position *"b"* in the second image can be determined quantitatively. In order to improve measurement accuracy in determining the flying velocities of the water droplets, a "sub-pixel interpolation" process, which is similar as that described in Hu et al. (1998) for PIV image processing, was used in the present study to locate the centers of the flying droplets at a sub-pixel level. Based on the statics of the measured flying velocity of the water droplets in the droplet stream, the standard deviation of the measured flying velocity of the mono-sized water droplets was found to be about 3.2 pixels, which is about 1.1 % of the displacement of the water droplets between the acquired phosphorescence image pair (i.e., averaged displacement of the water droplets given in Fig. 6 is 295.5 pixels). With the time delay between the acquired phosphorescence image pair known as $\Delta t = 1.1$ ms and the precalibrated scale ratio between the image plane and the object plane as that in Fig. 5b, the flying velocity of the water droplet "#*1*" can be calculated as $V = \overrightarrow{\Delta L}/\Delta t$. For example, for the test case shown in Fig. 6, the flying velocity of the preselected droplet "#*1*" was measured as $V = 2.01$ m/s.

3.3 Determination of the transient temperature of the in-flight droplets

After the corresponding positions of the in-flight droplets in the acquired phosphorescence image pair are determined, the intensity ratio of the same droplets in the two phosphorescence images can be used to calculate the phosphorescence lifetime of the 1-BrNp·Mβ-CD·ROH triplex molecules within the water droplets by using Eq. (3). With the calibration profile of the phosphorescence lifetime versus temperature as that shown in Fig. 3, the instantaneous temperature of the in-flight water droplet can be derived quantitatively from the acquired phosphorescence image pair. For the image processing of the lifetime-based MTT technique to calculate intensity ratio of the acquired phosphorescence pair (i.e., S1/S2), selecting the interrogation windows in the first and second phosphorescence images will be consistent with the scales of the water droplets to be measured. As shown theoretically in Eq. (2), since the intensity ratio of the acquired phosphorescence pair, thereby the lifetime of the phosphorescence emission, is only the function of the temperature of the tagged phosphorescent tracer molecules, the dynamic size change of the in-flight droplets due to evaporation would have no effect on the intensity ratio of the acquired phosphorescence pair. Figure 7 gives the phosphorescence intensity distributions of typical acquired phosphorescence images of the droplet stream (the black marks/circles on the images indicate the centers of the flying water droplets) along with the instantaneous temperature of the in-flight droplets derived from the phosphorescence image pair. As shown in Fig. 7, the instantaneous temperatures of the in-flight droplets in the center of the measurement window were found to be 11.9, 12.6 and 11.6 °C, respectively.

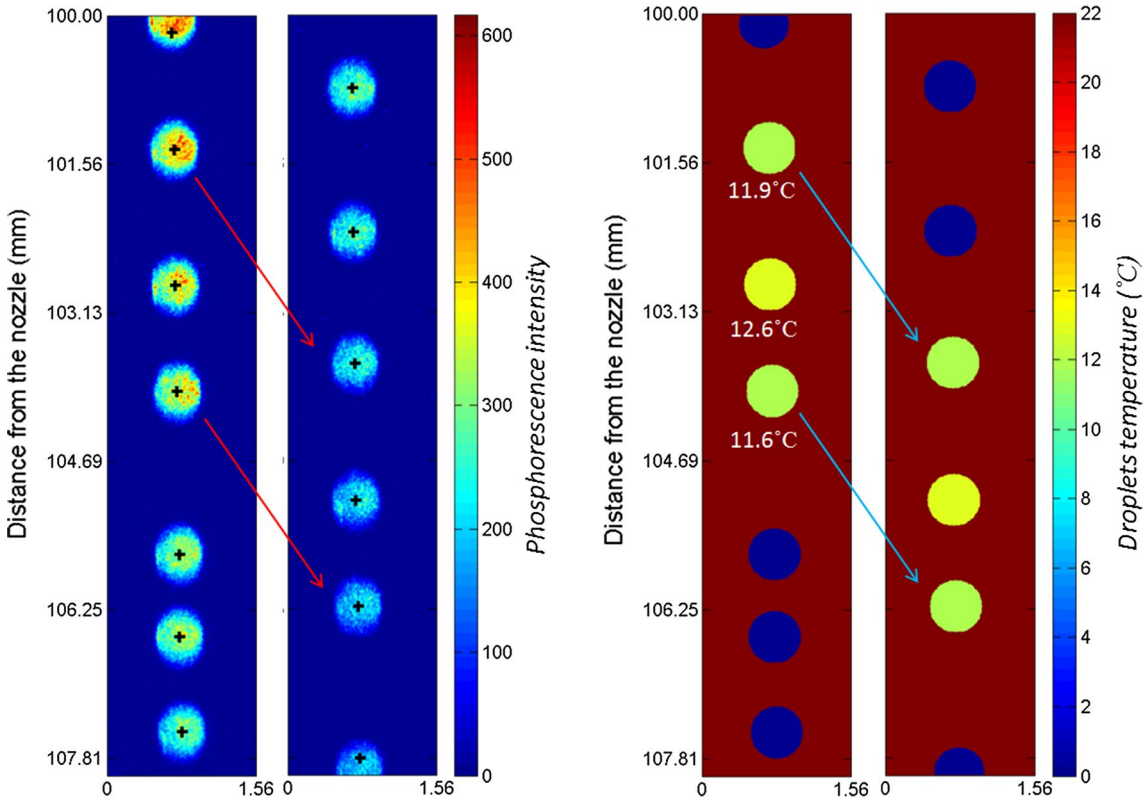

Fig. 7 Simultaneous measurements of droplet size, flying velocity and transient temperature of the in-flight droplets by using molecular tagging technique

Based on the time sequence of the measured instantaneous temperature distributions of the water droplets as those shown in Fig. 7, the dynamic and thermodynamics characteristics of the in-flight water droplets along their flying trajectories can be revealed quantitatively, which will be discussed in detail in the following sections.

3.4 Theoretical analysis on the unsteady heat transfer process between the in-flight droplets and ambient air

As described above, since the initial temperature of the water droplets out of the droplet generator was set to be lower than the temperature of ambient air, the small water droplets will be convectively heated up, while they fly through the ambient air. A theoretical analysis was performed in the present study by using a lumped capacitance method to examine the unsteady heat transfer process between the in-flight water droplets and the ambient air to predict the temperature variations of the in-flight droplets along their flying trajectories.

The following assumptions are made in the theoretical analysis to examine the unsteady heat transfer process between the in-flight water droplets and the ambient air:

1. The water droplets are assumed to keep their spherical shape while flying in the ambient air.
2. Negligible radiation effects due to the relatively low temperature of the water droplets.
3. Negligible small thermal resistance at the droplet surface, and negligible small temperature change in ambient air around the in-flight water droplet.
4. Since only the spatially averaged temperature of the water droplets is considered in the present study and the Biot number of the tiny water droplets (i.e., ~450 μm in diameter) considered here is very small (i.e., $Bi = h{\cdot}D/K \ll 0.1$), the in-flight water droplets are considered as isothermal spheres with the temperature differences within the micro-sized water droplets being neglected.

By using the lumped capacitance method described in the heat transfer textbook of Incropera and Dewitt (1996), the balance of the heat transfer in and out of a control volume around an in-flight water droplet can be expressed as:

$$-hA_s(T - T_\infty) = \rho \text{ Vol } C_p \frac{\mathrm{d}T}{\mathrm{d}t}, \tag{4}$$

where h is the convection coefficient of air around the surface of the in-flight water droplet; A_s is the surface area of the spherical droplet; T is the transient temperature of the in-flight droplet to be determined; T_∞ is the temperature of ambient air, which is a constant for the present study; ρ is the density of the water droplet, C_p is the specific heat of the droplet; Vol is the volume of the droplet; and t is the time after the water droplet leaves the droplet generator.

Introducing the temperature difference: $\theta = T - T_\infty$, and recognizing that $\frac{dT}{dt} = \frac{d\theta}{dt}$, Eq. (4) can be rewritten as:

$$\frac{\rho \,\mathrm{Vol}\, C_p}{hA_s}\frac{d\theta}{dt} = -\theta \tag{5}$$

Separating the variables and integrating from the initial condition, for which at $t = 0$ and $T = T_i$, it can be derived that

$$\frac{\rho\ \mathrm{Vol}\ C_p}{hA_s}\int_{\theta_I}^{\theta}\frac{d\theta}{\theta} = -\int_o^t dt \tag{6}$$

where $\theta_i = T_i - T_\infty$.

Evaluating the integral, it can be expressed as

$$\frac{\rho\ \mathrm{Vol}\ C_p}{hA_s}\ln\left(\frac{\theta_i}{\theta}\right) = t \tag{7}$$

or

$$\frac{\theta}{\theta_i} = \frac{T - T_\infty}{T_i - T_\infty} = \exp\left[-\left(\frac{hA_s}{\rho\ \mathrm{Vol}\ C_p}\right)t\right] \tag{8}$$

Since $\mathrm{Vol} = \frac{1}{6}\pi D^3$ and $A_s = \pi D^2$ for the present study, it can be derived that

$$T = \left[T_i - T_\infty + T_\infty \exp\left(\frac{6\,h\,t}{\rho D C_p}\right)\right] \Big/ \exp\left(\frac{6\,h\,t}{\rho D C_p}\right) \tag{9}$$

where D is the diameter of the water droplet.

The convection coefficient h is defined by

$$h = Nu_D\frac{k}{D}. \tag{10}$$

Where Nu_D is the Nusselt number and k is the thermal conductivity of air.

As described in Whitaker (1972), the Nusselt number Nu_D around a sphere in air can be expressed as

$$Nu_D = 2 + \left(0.4Re_D^{1/2} + 0.06Re_D^{2/3}\right)Pr^{0.4}\left(\frac{\mu}{\mu_s}\right)^{1/4} \tag{11}$$

where Re_D is the Reynolds number of the flying droplet in air, Pr is the Prandtl number, μ is the dynamic viscosity of air at T_i, and u_s is the mean dynamic viscosity of air during the droplet heating process.

The Reynolds number Re_D is defined as

$$Re_D = \frac{VD}{\upsilon} \tag{12}$$

where V is the flying velocity of the water droplet and υ is the kinematic viscosity of air.

Based on Eqs. (9–12) given above, the transient temperature of the in-flight water droplets along their flying trajectories can be predicted theoretically with the known droplet diameter D, flying velocity V, droplet initial temperature T_i and ambient air temperature T_∞.

3.5 Comparison of measurement results with the theoretical predictions

In the present study, a set of experiments were conducted to examine the unsteady heat transfer process between the in-flight water droplets and the ambient air at different test conditions. The molecular tagging technique described above was used to achieve simultaneous measurements of droplet size, velocity and temperature of the in-flight droplets. The measured temperature data were compared with the theoretical analysis results quantitatively to validate the measurement results. The measured temperature data were compared with the theoretical analysis results quantitatively to characterize the dynamic and thermodynamic behaviors of the in-flight droplets.

Since the experiment is designed mainly to demonstrate the implemented procedure of the molecular tagging technique, a relatively small temperature range (i.e., between 10 and 20 °C) was chosen for the experiment in order to simplify the experimental setup. During the experiments, while the ambient air temperature was kept constant at $T_\infty = 22$ °C, the initial temperature of the water droplet exhausted from the droplet generator exit was adjusted from $T_i = 11$–18 °C. The micro-sized water droplets were convectively heated up after they were exhausted from the droplet generator into the ambient air. The measurement window was set to locate at about 100 mm away from the exit of the droplet generator. As shown in Figs. 5, 6 and 7, the diameter of the water droplets exhausted from the droplet generator was measured to be about 450 μm with the flying velocity at about 2.01 m/s. It should be noted that the methodology of the molecular tagging technique is rather general and applicable for a much wider temperature range, depending on the molecular tracers and solutions used for the molecular tagging measurements (e.g., 0–100 °C for the phosphorescent triplex (1-BrNp·Mβ-CD·ROH) premixed in the water droplets).

Based on 50 frames of the instantaneous measurements as those shown in Fig. 7, the averaged temperature of the micro-sized in-flight water droplet at the center of the measurement window was calculated. Figure 8 shows the measured temperature of the in-flight water droplets at

100 mm away from the droplet generator as a function of the initial temperature of the water droplets. The error bars given in the plot represent the standard deviation values based on the 50 frames of instantaneous temperature measurements at each test condition. The predicted temperature values of the in-flight droplets at different test conditions were also given in the same plot for quantitative comparison. The predicted temperature values were obtained based on the theoretical analysis procedure described above (i.e., in Sect. 3.3) with the measured droplet size (i.e., 450 μm in diameter), droplet flying velocity (i.e., $V = 2.01$ m/s in flying velocity) and the initial temperature of the water droplets measured at the exit of the droplet generator (i.e., $T_i = 11$–18 °C) as the input parameters. As shown in Fig. 8, the measured temperatures of the in-flight droplets were found to agree well in general with the theoretically predicted values. The differences between the measured droplet temperatures and the predicted values were found to be within 0.5 °C, which is comparable to the standard derivation values (i.e., indicated as the error bars in the plot) of the instantaneous temperature measurements.

In the present study, the temperature variations of the in-flight water droplets as a function of the flying time in ambient air were also investigated by moving the measurement window further away from the exit of the droplet generator. During the experiments, the ambient air temperature was kept constant at $T_\infty = 22$ °C, and the initial temperature of the water droplet exhausted from the droplet generator exit was set at $T_i = 11$ °C. Figure 9 shows the measured temperatures of in-flight water droplets at different time after exhausted from the exit of the droplet generator in comparison with the theoretical predictions. As expected, the temperature of the in-flight water droplets was found to increase monotonically with the increasing flying time in the ambient air due to the convective heat transfer between the in-flight water droplets and the ambient air. While the measured temperature data and the predicted results show a similar tendency as the flying time increases, the rate of increase in the measured temperature data was found to be slightly higher than that of the theoretical predictions. As a result, the differences between the measured temperature data and the predicted results were found to increase gradually as the flying time increases. The maximum difference between the measured temperature data and the predicted results was found to be about 0.80 °C with the micro-sized water droplets flying about 0.2 s after exhausted from the exit of the droplet generator. It should be noted that, in addition to the measurement uncertainty, the simplified theoretic model that neglects the thermal gradients within the water droplets can also contribute the differences between the theoretic predictions and the measurement results.

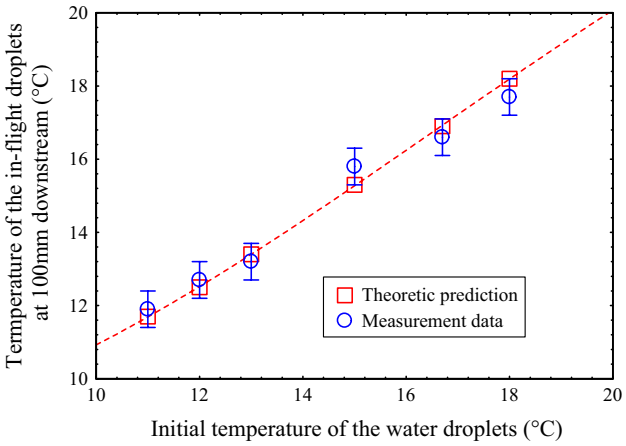

Fig. 8 The temperature of the in-flight droplets at 100 mm away from the droplet generator as a function of the initial temperature of the water droplets

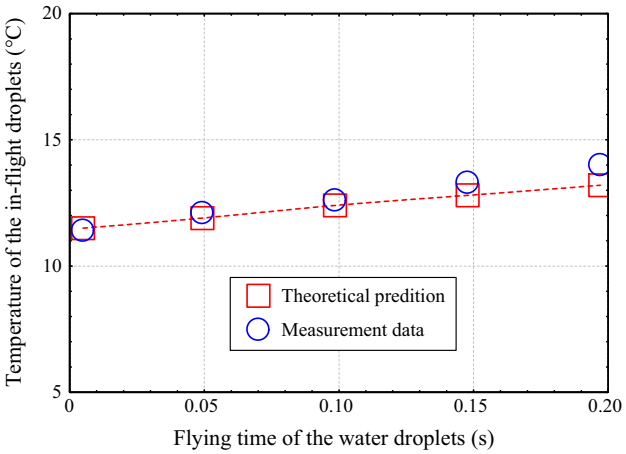

Fig. 9 The measured temperature of the in-flight droplets as a function of flying time

4 Summary

We presented the progress made in developing a molecular tagging technique for achieving simultaneous measurements of droplet size, flying velocity and transient temperature of in-flight liquid droplets. Phosphorescent 1-BrNp·Mβ-CD·ROH triplex molecules, which can be turned into long-lasting glowing marks upon excitation by photons of appropriate wavelength, were used as the molecular tracers for the quantitative measurements. A pulsed UV laser was used to "tag" the phosphorescent triplex molecules premixed within in-flight droplets to emit long-lived LIP. After the same laser excitation pulse, the tagged phosphorescent triplex molecules were imaged at two successive times within the phosphorescent lifetime of

the tracer molecules. While the size of the in-flight droplets was determined quantitatively based on the acquired droplet images with a precalibrated scale ratio between the image plane and the object plane, the displacements of the droplets between the two image acquisitions were used to estimate the flying velocity of the in-flight droplets. The transient temperature of the in-flight droplets was derived simultaneously by taking advantage of the temperature dependence of the phosphorescence lifetime, which is estimated from the phosphorescence intensity ratio of the two interrogations.

The feasibility and implementation of the molecular tagging technique were demonstrated by conducting simultaneous measurements of droplet size, flying velocity and transient temperature of micro-sized water droplets exhausted from a piezoelectric droplet generator at different test conditions. During the experiments, while the ambient air temperature was kept constant at 22 °C, the initial temperature of the micro-sized water droplet at the droplet generator exit was set at a lower temperature range from 11 to 18 °C. After injected into the ambient air, the micro-sized water droplets were convectively heated up as they flew through the ambient air, which caused the transient temperature of the micro-sized water droplets to vary dynamically along their flight trajectories. The unsteady heat transfer process between the in-flight water droplets and the ambient air was also analyzed theoretically by using the lumped capacitance method to predict the temperature of the in-flight water droplets along their flight trajectories. The measured temperature data were compared quantitatively with the theoretical analysis results, and the discrepancies between the measured temperature data and the theoretical prediction results were found to be within 0.80 °C.

Acknowledgments The authors want to thank Dr. M.M. Koochesfahani of Michigan State University for the technical help pertinent to the present study. The funding support from National Science Foundation program under award numbers of CBET-1064196 and CBET-1435590 and Iowa Regents Innovation Fund (RIF) program is also gratefully acknowledged.

References

Castanet G, Lavieille P, Lemoine F et al (2002) Energetic budget on an evaporating monodisperse droplet stream using combined optical methods. Int J Heat Mass Transf 45:5053–5067. doi:10.1016/S0017-9310(02)00204-1

Coppeta J, Rogers C (1998) Dual emission laser induced fluorescence for direct planar scalar behavior measurements. Exp Fluids 25:1–15. doi:10.1007/s003480050202

Ferraudi GJ (1988) Elements of inorganic photochemistry. Wiley-Interscience, New York

Gendrich C, Koochesfahani M, Nocera D (1997) Molecular tagging velocimetry and other novel applications of a new phosphorescent supramolecule. Exp Fluids 23:361–372

González JE, Black WZ (1997) Study of droplet sprays prior to impact on a heated horizontal surface. J Heat Transf 119:279. doi:10.1115/1.2824221

Hall DD, Mudawar I (1995) Experimental and numerical study of quenching complex-shaped metallic alloys with multiple, overlapping sprays. Int J Heat Mass Transf 38:1201–1216. doi:10.1016/0017-9310(94)00244-P

Hartmann W, Gray M, Ponce A (1996) Substrate induced phosphorescence from cyclodextrin·lumophore host-guest complexes. Inorg Chim Acta 234:239–248

Hopkins RJ, Symes R, Sayer RM, Reid JP (2003) Determination of the size and composition of multicomponent ethanol/water droplets by cavity-enhanced Raman scattering. Chem Phys Lett 380:665–672. doi:10.1016/j.cplett.2003.09.048

Hu H, Huang D (2009) Simultaneous measurements of droplet size and transient temperature within surface water droplets. AIAA J 47:813–820

Hu H, Jin Z (2010) An icing physics study by using lifetime-based molecular tagging thermometry technique. Int J Multiph Flow 36:672–681

Hu H, Koochesfahani M (2003) A novel technique for quantitative temperature mapping in liquid by measuring the lifetime of laser induced phosphorescence. J Vis 6:143–153

Hu H, Koochesfahani MM (2006) Molecular tagging velocimetry and thermometry and its application to the wake of a heated circular cylinder. Meas Sci Technol 17:1269–1281. doi:10.1088/0957-0233/17/6/S06

Hu H, Koochesfahani MM (2011) Thermal effects on the wake of a heated circular cylinder operating in mixed convection regime. J Fluid Mech 685:235–270. doi:10.1017/jfm.2011.313

Hu H, Saga T, Kobayashi T, Okamoto T, Taniguchi N (1998) Evaluation of cross correlation method by using PIV standard images. J Vis 1(1):87–94

Hu H, Koochesfahani M, Lum C (2006) Molecular tagging thermometry with adjustable temperature sensitivity. Exp Fluids 40:753–763

Hu H, Jin Z, Koochesfahani M, Nocera D (2010) Experimental investigations of micro-scale flow and heat transfer phenomena by using molecular tagging techniques. Meas Sci Technol 21:085401 **(14 pp)**

Incropera F, DeWitt D (1996) Introduction to heat transfer. Wiley, New York

Kim HJ, Kihm KD, Allen JS (2003) Examination of ratiometric laser induced fluorescence thermometry for microscale spatial measurement resolution. Int J Heat Mass Transf 46:3967–3974. doi:10.1016/S0017-9310(03)00243-6

Lavieille P, Lemoine F, Lavergne G, Lebouché M (2001) Evaporating and combusting droplet temperature measurements using two-color laser-induced fluorescence. Exp Fluids 31:45–55. doi:10.1007/s003480000257

Lemoine F, Castanet G (2013) Temperature and chemical composition of droplets by optical measurement techniques: a state-of-the-art review. Exp Fluids 54(7):1572

Mochizuki T, Nozaki T, Mori YH, Kaji N (1999) Heat transfer to liquid drops passing through an immiscible liquid medium between tilted parallel-plate electrodes. Int J Heat Mass Transf 42:3113–3129. doi:10.1016/S0017-9310(98)00381-0

Müller T, Grünefeld G, Beushausen V (2000) High-precision measurement of the temperature of methanol and ethanol droplets using spontaneous Raman scattering. Appl Phys B 70(1):155–158

Nozaki T, Mochizuki T, Kaji N, Mori YH (1995) Application of liquid-crystal thermometry to drop temperature measurements. Exp Fluids 18:137–144. doi:10.1007/BF00230257

Omrane A, Juhlin G, Ossler F, Aldén M (2004a) Temperature measurements of single droplets by use of laser-induced phosphorescence. Appl Opt 43:3523–3529

Omrane A, Santesson S, Alden M, Nilsson S (2004b) Laser techniques in acoustically levitated micro droplets. Lab Chip 4:287–291. doi:10.1039/b402440k

Ramamurthy V, Schanze KS (1998) Organic and inorganic photochemistry. Mol Supramol Photochem viii:355

Richards CD, Richards RF, Boltzman S (1998) Transient temperature measurements in a convectively cooled droplet. Exp Fluids 25(5):392–400

Saga T, Kobayashi T, Segawa S, Hu H (2001) Development and evaluation of an improved correlation based PTV method. J Vis 4:29–37. doi:10.1007/BF03182453

Salazar VM, González JE, Rivera LA (2004) Measurement of temperatures on in-flight water droplets by laser induced fluorescence thermometry. J Heat Transf 126:279. doi:10.1115/1.1667527

Schulz C, Sick V (2005) Tracer-LIF diagnostics: quantitative measurement of fuel concentration, temperature and fuel/air ratio in practical combustion systems. Prog Energy Combust Sci 31:75–121. doi:10.1016/j.pecs.2004.08.002

Schweiger G (1990) Raman scattering on single aerosol particles and on flowing aerosols: a review. J Aerosol Sci 21:483–509. doi:10.1016/0021-8502(90)90126-I

Tuckermann R, Bauerecker S, Cammenga HK (2005) IR-thermography of evaporating acoustically levitated drops. Int J Thermophys 26:1583–1594. doi:10.1007/s10765-005-8105-6

Van Beeck JP, Riethmuller ML (1995) Nonintrusive measurements of temperature and size of single falling raindrops. Appl Opt 34:1633–1639. doi:10.1364/AO.34.001633

Van Beeck JP, Giannoulis D, Zimmer L, Riethmuller ML (1999) Global rainbow thermometry for droplet-temperature measurement. Opt Lett 24:1696–1698. doi:10.1364/OL.24.001696

Vetrano MR, Gauthier S, van Beeck J et al (2005) Characterization of a non-isothermal water spray by global rainbow thermometry. Exp Fluids 40:15–22. doi:10.1007/s00348-005-0042-4

Whitaker S (1972) Forced convection heat transfer correlations for flow in pipes, past flat plates, single cylinders, single spheres, and for flow in packed beds and tube bundles. AIChE J 18:361–371. doi:10.1002/aic.690180219

Wilms J, Gréhan G, Lavergne G (2008) Global rainbow refractometry with a selective imaging method. Part Part Syst Charact 25:39–48. doi:10.1002/ppsc.200700006

Wulsten E, Lee G (2008) Surface temperature of acoustically levitated water microdroplets measured using infra-red thermography. Chem Eng Sci 63:5420–5424. doi:10.1016/j.ces.2008.07.020

Zhang Y, Zhang G, Xu M, Wang J (2013) Droplet temperature measurement based on 2-color laser-induced exciplex fluorescence. Exp Fluids 54:1583. doi:10.1007/s00348-013-1583-6